

# Noise Analysis of Solid-Core Polarization-Maintaining Photonic Interferometer Fiber Optic Gyroscope

Shisen DU\*, Zuoming SUN, Zhonggang ZHANG, and Chunxi ZHANG

*School of Instrument Science and Opto-electronics Engineering, Beihang University, Beijing 100191, China*

(Received November 17, 2010; Accepted February 15, 2011)

We report the prediction of the random walk coefficient of a solid-core single-mode polarization-maintaining photonic interferometer fiber optic gyroscope, a novel sensor that exhibits reduced thermal sensitivity owing to the stable temperature coefficient use of a photonic fiber. The random walk coefficient of the photonic interferometer fiber optic gyroscope is limited by detector thermal noise for detected powers under  $1\ \mu\text{W}$  and excess noise above  $1\ \mu\text{W}$ . Above this power level, the random walk coefficient is found to be independent of detected power and asymptotically to be  $0.0029^\circ/\sqrt{\text{h}}$ . This result is verified by the experiment. © 2011 The Japan Society of Applied Physics

**Keywords:** photonic polarization maintaining fiber, IFOG, random walk coefficient, noise, excess noise

## 1. Introduction

The interferometer fiber optic gyroscope (IFOG) has proven to be one of the most successful fiber sensor technologies,<sup>1)</sup> but current IFOGs are limited by several sources of error. These include excess source noise from broadband light and fluctuations in the source mean wavelength, resulting in instability in the IFOG scale factor.<sup>2)</sup>

The polarization-maintaining photonic crystal fiber (PCF) is emerging as a new competitor of the traditional polarization-maintaining fiber.<sup>3)</sup> One of the potential applications of this photonic crystal fiber is as one of the enabling technologies of the next generation of IFOG instruments. The recent advent of a photonic crystal fiber with a relatively low loss (4 dB/km) offers a radically new means for further reducing the complexity, size, and thermal sensitivity of existing FOGs.<sup>4)</sup> There are several key advantages of the PCF for IFOG applications:<sup>5)</sup> (1) PCF remains in the single mode and thus can transmit polarized light in a broad range of frequencies, (2) PCF has a shorter beat length than the common PMF, thus it reduces bend-induced coupling between polarization states and improves the extinction rate, and (3) PCF presents a more stable temperature coefficient of birefringence.

Kim *et al.* have recently confirmed some of these advantages through their demonstration of the first experimental air-core fiber gyro.<sup>6)</sup> In 2007, Blin *et al.* found that random walk of air-core fiber gyro is comparable to that of a conventional FOG with a similar scale factor;<sup>7)</sup> they also found that a 6.5-fold reduction in thermal sensitivity can be demonstrated experimentally in a photonic-band gap fiber-optic gyroscope, compared with the same gyro operated with a similar coil of conventional fiber in the same year.<sup>8)</sup> Digonnet *et al.* measured the coherent backscattering noise in a photonic-band gap fiber optic gyroscope, and revealed that the photonic-band gap fiber optic gyroscope has a low sensitivity to the Kerr effect but exhibits stronger backscattering.<sup>9)</sup> In this work, we study the random walk

coefficient of a solid-core single-mode polarization-maintaining photonic crystal interferometer fiber optic gyroscope (PCF-IFOG). Before declaring the advantage of PCF-IFOG over conventional FOGs it is necessary to understand the limitations of PCF-IFOG performance. We attempt to gain such an understanding empirically. We report the results of noise studies performed with PCF-IFOG.

## 2. Experimental PCF-IFOG

A scanning electron microscope image of the solid-core single-mode polarization-maintaining PCF cross section is shown in Fig. 1. This photonic crystal fiber combines a high birefringence with a single material, silica. The single-mode polarized light travels mostly in the silica, the refractive index of the fiber has a more stable temperature coefficient of birefringence, and the Shupe effect is substantially reduced.

Figure 2 is a diagram of the experimental photonic interferometer fiber gyro. It uses a Sagnac interferometer made of a loop of 800 m of PCF produced by YOFC, coiled in a quadrupolar winding. The experimental photonic interferometer fiber gyro includes a broad band light source (SFS), and a 3 dB coupler that enables the characterization of the fiber both in transmission and reflection. 30 to 40 mW of optical power from a standard SFS was launched into the fiber. Light from the SFS is sent through a fiber coupler, then split by a 3 dB integrated optic chip (IOC) and coupled into the coil in both the clockwise and counterclockwise directions. Each of the two IOC output ports is pigtailed to a 1 m length of conventional fiber, terminated at an angle to reduce back reflection, and coupled to one end of the PCF sensing coil. After traveling around the loop, the signals return to and interfere at the coupler. Through the Sagnac effect, this interference yields an output signal power that depends on the rotation rate imparted to the coil. The interferometer was biased for maximum sensitivity with a fiber-pigtailed integrated optic chip placed in the loop and operated at the proper loop frequency. The output signal from the reciprocal port of the 3 dB fiber coupler was detected with a detector. Both the fundamental frequency f

\*E-mail address: shisendu@msn.com

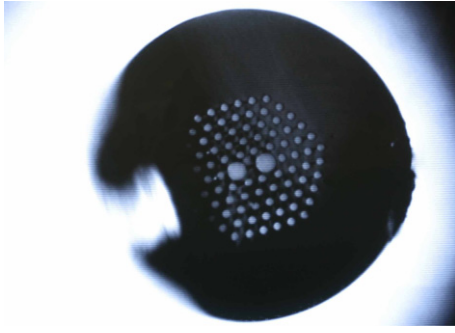


Fig. 1. (Color online) Scanning electron microscope image of polarization-maintaining PCF.

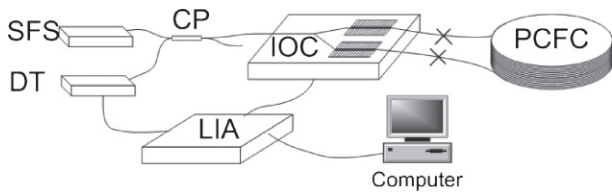


Fig. 2. Configuration of photonic interferometer fiber gyroscope; CP: coupler; IOC: integrate optic chip; PCFC: photonic crystal fiber coil; DT: detector, LIA: lock-in amplifier.

and the second-harmonic frequency  $2f$  of the detected electrical signal were extracted with a lock-in amplifier and recorded on a computer.

### 3. Theory and Analysis

The basic sensitivity of the phase shift  $\phi_s$  to the rotation rate is the Sagnac scale factor, given by the quantity  $G$  in

$$\phi_s = G\Omega = \frac{2\pi LD}{\lambda c} \Omega, \quad (1)$$

where  $L$  and  $D$  are the length and average diameter of the fiber coil, respectively,  $\lambda$  is the source wavelength,  $c$  is the speed of light in vacuum, and  $\Omega$  is the rotation rate in radians per second. For fiber length of  $L = 800$  m, diameter of  $D = 65$  mm, and  $\lambda = 1550$  nm,  $G = 0.7 \text{ s}^{-1}$ .

For a given source power  $P_0$  out of the source pigtail, the detector power is given by

$$P_d = P_0 10^{-(A_c + aL)/10}, \quad (2)$$

where  $a$  is the fiber loss in decibels per meter, and  $A_c$  includes all other circuit losses due to the fiber couplers, polarizer, IOC and its pigtail, and splices. Splicing PCF to PM fibers induces more loss than splicing PM to PM fibers; if  $A_c$  is assumed to be 24 dB and  $P_0$  is 10 mW, the detector power will be 160  $\mu\text{W}$ . Equations for each of these noise sources are listed next. Shot noise is<sup>10)</sup>

$$\sum_S = \frac{1}{G} \left( \frac{2q}{R_d P_d} \right)^{0.5}, \quad (3)$$

where  $q = 1.6 \times 10^{-19}$  coulomb, and  $R_d$  is the responsivity of the detector (0.9 A/W). Excess noise is<sup>11)</sup>

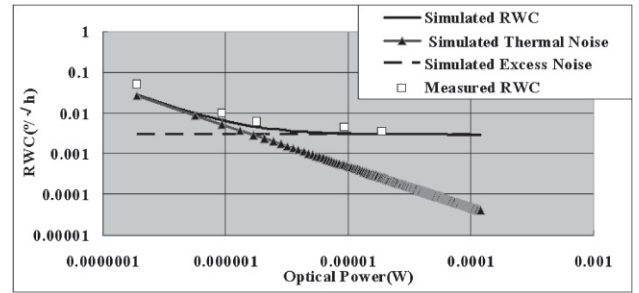


Fig. 3. Simulated random walk coefficient as a function of average detected power.

$$\sum_X = \frac{1}{G} \left( \frac{1}{\Delta\nu} \right)^{0.5}, \quad (4)$$

where the effective bandwidth is

$$\Delta\nu = \left( \frac{\pi}{8 \ln 2} \right)^{0.5} \frac{c \Delta\lambda_{\text{FWHM}}}{\lambda_0^2}, \quad (5)$$

and  $\Delta\lambda_{\text{FWHM}}$  is the half-power line width of a Gaussian source spectrum. An estimated value of 30 nm can be assumed for a typical SFS. Detected thermal noise is

$$\sum_E = \frac{1}{G} \frac{\text{NEP}}{P_d}, \quad (6)$$

where the NEP of a typical InGaAs p-i-n photodiode is 1.0 pW/Hz<sup>0.5</sup>. Total RWC is

$$\sum_{\text{TOT}} = \left( \sum_S^2 + \sum_X^2 + \sum_E^2 \right)^{0.5}. \quad (7)$$

In Fig. 3, the random walk measured by this process is plotted as filled circles as a function of the average detected power. For low detection powers ( $< 1 \mu\text{W}$ ), the RWC is inversely proportional to power, and the main noise to the RWC is the electronic noise. At higher powers ( $> 1 \mu\text{W}$ ), the sensitivity levels off asymptotically to a random walk coefficient of  $0.0029^\circ/\sqrt{\text{h}}$ . This value is comparable to the minimum detectable phase of a conventional FOG.

In addition to RWC testing, the bias drift test of the PCF coil is performed. The test is run for a minimum of 4 h. The integration time for the test is 1 s. The 14400 s data set is analyzed with the standard Allan variance routine and the resulting data plot is shown in Fig. 4.<sup>12)</sup> As can be seen in Fig. 4, the 800 m PCF coil exhibited  $0.0029^\circ/\text{hr}$  performance when the detected power was about 20  $\mu\text{W}$ . From the Allan variance plot in Fig. 4, we fit the measured data by the least-squares method. We obtain the angle random walk  $^\circ/\sqrt{\text{h}}$ , bias instability  $^\circ/\text{h}$ , and rate random walk  $^\circ/\text{h}^{1.5}$  after fitting the measured data. The noise coefficients are read off and shown in Table 1.

These theoretical noise limits are plotted in Fig. 3 with the parameters of our experimental PCF-IFOG. For powers below 1  $\mu\text{W}$ , the thermal noise is the main limitation, while the excess noise is dominant for powers above 1  $\mu\text{W}$ . The overall contribution of all noise sources (square root of the sum of the squared individual contributions) is also plotted

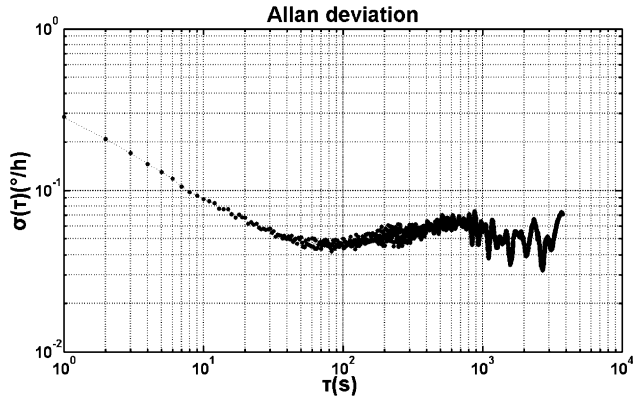


Fig. 4. Plot of Allan variance analysis results.

Table 1. Overview of Allan variance of PCF-IFOG.

Parameter	Value
Random walk coefficient	0.0029 ( $^{\circ}/\sqrt{\text{h}}$ )
Bias instability	0.042 ( $^{\circ}/\text{h}$ )
Rate of random walk	0.288 ( $^{\circ}/\text{h}^{1.5}$ )

in Fig. 3 (solid curve). This theoretical detection limit agrees well with the experimental result. This agreement demonstrates unambiguously that the noise of the PCF-IFOG is limited by excess noise. This comparison also confirms that the minimum random walk of this PCF-IFOG is  $0.0029^{\circ}/\sqrt{\text{h}}$ .

#### 4. Conclusions

The Allan variance technique was successfully applied to PCF-IFOG data. The result clearly shows that shot noise, excess noise, and detected thermal noise are the dominant error sources present in the characterized PCF-IFOG.

In conclusion, we have shown that the RWC of a PCF-IFOG is limited by the thermal noise at low detected power

( $<1\mu\text{W}$ ) and excess noise at higher power ( $>1\mu\text{W}$ ). The RWC of this PCF-IFOG was as low as  $0.0029^{\circ}/\sqrt{\text{h}}$ , which is comparable to the RWC of a conventional IFOG. This performance was a result of the increase in source power to reach the excess-noise limit, which originated from the higher loss of the fiber and the splicing of PCF to PM fibers. This disadvantage will disappear should a PCF with reduced loss be produced in the future, and used to fabricate the IOC. As the solid-core photonic fiber fabrication technology improves, the PCF cost will be reduced to a level comparable to that of conventional polarization-maintaining fibers, and the PCF-IFOG will offer the potential to be one of the enabling technologies of the next generation of IFOG instruments.

#### References

- 1) H. Lefèvre: *The Fiber-Optic Gyroscope* (Artech, Norwood, MA, 1993) p. 2.
- 2) K. Killian, M. Burmenko, and W. Hollinger: Proc. SPIE **2292** (1994) 255.
- 3) A. Michie, J. Canning, W. Padden, K. Lyttikäinen, M. Åslund, and J. Digweed: Proc. SPIE **5855** (2005) 614.
- 4) J. Tawney, F. Hakimi, R. L. Willig, J. Alonzo, R. T. Bise, F. DiMarcello, E. M. Monberg, T. Stockert, and D. J. Trevor: Proc. Optical Fiber Sensors, 2006, OSA Tech. Dig., ME8 (CD-ROM).
- 5) J. Ju, L. Ma, and W. Jin: Proc. SPIE **7503** (2009) 75035B.
- 6) H. K. Kim, V. Dangui, M. Dignonnet, and G. Kino: Proc. SPIE **5855** (2005) 198.
- 7) S. Blin, M. J. F. Dignonnet, and G. S. Kino: J. Lightwave Technol. **19** (2007) 1520.
- 8) S. Blin, H. K. Kim, and M. J. F. Dignonnet: J. Lightwave Technol. **25** (2007) 861.
- 9) M. J. F. Dignonnet, S. W. Lloyd, and S. Fan: Proc. SPIE **7503** (2009) 750302.
- 10) W. K. Burns and R. P. Moeller: Proc. SPIE **3937** (1996) 381.
- 11) W. K. Burns, R. P. Moeller, and A. Dandridge: IEEE Photonics Technol. Lett. **2** (1999) 606.
- 12) IEEE Std 952-1997 (2008).